

Measurement of atomic polarizabilities using Floquet spectroscopy

Y. Zhang, M. Ciocca, L.-W. He, C. E. Burkhardt, and J. J. Leventhal
Department of Physics, University of Missouri—St. Louis, St. Louis, Missouri 63121
 (Received 13 December 1993)

The complex network of Floquet states that results from an application of an external ac electric field to a collection of atoms is investigated. It is shown that precision dc Stark spectroscopy can reveal the details of the quasienergy states, Floquet states, spawned by the application of a rf field. Transitions to the Floquet sidebands of quadratic (dc) Stark states are found to have absorption intensities in good agreement with theory. This combination of dc and ac fields applied to atoms, Floquet spectroscopy, is then used to determine accurately the scalar and tensor polarizabilities of the $65p^2P$ state of sodium. Deviations from quadratic behavior are investigated as well as the relationship of our measured polarizability to previous measurements at lower principal quantum numbers.

PACS number(s): 32.30.Bv, 32.60.+i, 32.80.-t

INTRODUCTION

The demand for increased precision in measurements of atomic parameters that has resulted from the development of highly sophisticated calculation techniques has, fortunately, been accompanied by the availability of the laser as a laboratory tool. These factors have led to the invention of a number of new spectroscopic techniques, many of which exploit the extreme sensitivity of highly excited Rydberg atoms to measure effects that would be difficult or impossible to detect using atoms in lower-lying excited states [1]. The Rydberg atoms are often produced by two-step laser excitation, in which case the accuracy of the measured atomic parameters is limited by the bandwidth, typically $\sim 0.1\text{--}3\text{ cm}^{-1}$, of the laser that provides the final step in the excitation sequence. Further, because the spacing of adjacent levels decreases with increasing principal quantum number n , measurements have, for the most part, been confined to atoms for which n is less than about 40. Correlations with scaling laws for the atomic parameters have thus been similarly restricted. Recently, we reported the results of experiments [2] which employed a novel three-step excitation sequence, the last step of which was provided by a line selectable CO_2 laser of bandwidth $\sim 50\text{ kHz}$ ($\sim 2\text{ }\mu\text{cm}^{-1}$). Using this method, precision (dc) Stark spectroscopy, we obtained atomic parameters such as term energies and quantum defects with unprecedented accuracy. We were also able to access states having $n \geq 40$ with relative ease.

Using precision Stark spectroscopy as a foundation, we have developed yet another method for measuring atomic parameters. We refer to this method, which employs both the ac and the dc Stark effects, as Floquet spectroscopy. The ac field employed is of radio frequency (rf), which can be measured with extremely high accuracy and precision. Coupled with the improved term energies that we measured using precision dc Stark spectroscopy [2], Floquet spectroscopy yields other parameters with greater precision than any previous measurements. Moreover, the range of n that may be studied is extended to ~ 100 . As will be shown, a unique advantage of Flo-

quet spectroscopy over precision dc Stark spectroscopy is that it can provide many more data points for a given measurement because the rf frequency can be varied continuously. Thus a detailed energy-level diagram can be constructed. For example, it is possible to trace the evolution of a (field-free) nondegenerate dc Stark state from the low-field region in which the energy is proportional to the square of the field strength to higher fields at which it mimics an excited state of hydrogen and exhibits linear behavior.

The essence of Floquet spectroscopy is the ac Stark [3] effect on the Rydberg atoms that result from immersion in the rf field. Imposition of this field produces an intricate network of states superposed on each stationary state of the atom [4]. The nature of these new states, which are necessarily solutions of the time-dependent Schrödinger equation, depends upon the frequency ω and amplitude G of the ac field as well as the characteristics of the stationary states. Such states are often referred to as quasienergy, dressed, or Floquet states. Their eigenvalues are $E_{n,k} = E_n + k\hbar\omega$ (k an integer), where E_n is the eigenvalue of the progenitor (stationary) state, that is, the corresponding eigenstate $R_n(\mathbf{r})$ of the time-independent atomic Hamiltonian. These eigenstates may be truly zero-field atomic states or, as in Floquet spectroscopy, they may be dc Stark states.

In the work reported here we use Floquet spectroscopy to probe the nature of the arrays of dressed states that arise from the ac Stark effect on stationary dc Stark states that are nondegenerate in zero field. We compare the results, including absorption intensities, with those expected from solution of the time-dependent Schrödinger equation. To illustrate the power of Floquet spectroscopy we trace the dc Stark shifts of these states as they undergo a metamorphosis from quadratic toward linear dependence on the dc field strength. In so doing, we measure the scalar and tensor polarizabilities of $\text{Na}(65p^2P)$ and compare the result with scaled values of lower n . In addition, although we are able to resolve completely all fine-structure levels, we obtain a value of the fine-structure interval that is in good agreement with interval scaling law.

APPARATUS

The atomic beam apparatus used in these experiments has been described in detail elsewhere [2]. The experiments were performed by irradiating a beam of sodium atoms, density $\sim 10^7 \text{ cm}^{-3}$, by three laser beams at the center of a pair of Stark plates as shown in Fig. 1. The fields were applied to the Stark plates so that the dc and rf fields were parallel.

Two 10-Hz pulsed beams, produced by grazing incidence dye laser and pumped by a single Nd:YAG laser (where YAG denotes yttrium aluminum garnet), were used to excite the atoms to the $12s^2S$ intermediate state via $\text{Na}(3p^2P_{3/2})$. The third laser, a cw line-selectable CO_2 laser tuned to the $10P(24)$ line ($940.54809 \text{ cm}^{-1}$ per photon), placed the total laser energy, the three photon energy, slightly higher than that of the $65p^2P$ states. The gain curve of the CO_2 laser is $\sim 100 \text{ MHz}$ wide, so that, although tuned manually to the maximum of the gain curve when data were acquired, there is roughly $\pm 10 \text{ MHz}$ uncertainty in the energy of the photons from the CO_2 laser. This uncertainty, coupled with the uncertainty of the $12s^2S$ energy, limits the precision to which the energy difference between the three-photon energy and the $65p^2P$ states is known to roughly $\pm 20 \text{ MHz}$, 0.0007 cm^{-1} . Nevertheless, the narrow bandwidth of the CO_2 laser line, $\sim 50 \text{ kHz}$, permitted selective excitation in the region of the closely packed states for $n \approx 64$.

Two polarization schemes were employed. In one, all three laser beams were plane polarized in the direction of the electric fields, thus ensuring excitation to states that would be designated $J=3/2$, $M_J=\pm 1/2$ in the absence of external fields ($\Delta J \neq 0$ if $\Delta M_J = 0$). The other polarization scheme was identical to the first except the CO_2 laser beam was circularly polarized. For these experiments the final states were either $J=3/2$ or $1/2$ with $M_J=1/2$ or $3/2$.

Data may be acquired with or without the rf field present. In either case the dc field F was scanned with the three laser beam frequencies fixed. The value of F was set prior to each laser pulse and increased $\sim 5 \mu\text{s}$ after the pulse to a value sufficient to field ionize atoms that had absorbed a photon from each of the three laser beams, but not atoms in the $12s^2S$ intermediate state. The ions were then detected by conventional methods. An F spectrum, F vs ion signal, was thus assembled. Such spectra represent the probability of absorption by an atom of photons from all three laser beams, an energy we shall refer to as the three photon energy, as a function

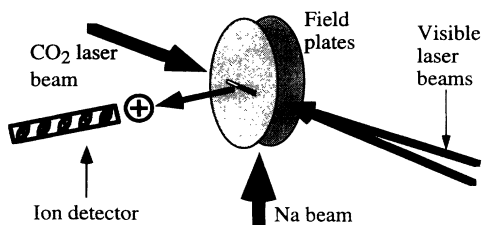


FIG. 1. Schematic diagram of the apparatus.

of F . The three-photon absorption can occur because application of F Stark shifts the high-lying atomic levels into resonance with the three-photon energy. The intermediate states are virtually unaffected by these low fields.

As will be shown, application of the rf field, together with the dc field, produces an intricate network of Floquet states, the nature of which may be probed with an F spectrum. In this case, detection of ions still signifies absorption of the three photon energy by the atoms, one photon from each laser beam. Excitation to a Floquet state not present in the absence of the rf field may be viewed as occurring with additional absorption, or stimulated emission, of one or more "rf photons." Nevertheless, in these experiments, the reference energy is most conveniently viewed as the three-photon energy, meaning one photon from each laser beam.

THEORY

The Hamiltonian of the system may be written in the form

$$\mathcal{H} = \mathcal{H}_a + \mathcal{H}_S, \quad (1)$$

where \mathcal{H}_a is the atomic Hamiltonian and \mathcal{H}_S contains the effects of the external fields. The solutions of the Schrödinger equation are quite different for the cases in which the progenitor states are degenerate and nondegenerate. In this work we consider only nondegenerate states for which there is no permanent electric dipole moment and \mathcal{H}_S is given by

$$\mathcal{H}_S = -\frac{1}{2}\alpha\mathcal{E}^2, \quad (2)$$

where \mathcal{E} is the electric field and α is a constant that is a linear combination of the scalar and tensor polarizabilities, α_0 and α_2 , that depends on the particular angular momentum level. At low fields the dc Stark states are very nearly quadratic, justifying the assumption that α is a constant. At higher fields the behavior must deviate from F^2 dependence because the dc Stark state must join the linear hydrogenic manifold [5,6]. As will be shown below, Floquet spectroscopy can be used to measure α_0 and α_2 as well as to measure the deviations from quadratic behavior. Of course, as the field is increased, all "quadratic" Stark states must join the nearest hydrogenic manifold and exhibit linear behavior, at least until perturbed by states from adjoining manifolds.

The dc field is F and the rf electric field is given by $G \cos(\omega t)$, where ω is the rf frequency. The electric field is then given by

$$\mathcal{E} = F + G \cos(\omega t). \quad (3)$$

Since F and G are collinear in these experiments we may write

$$\begin{aligned} \mathcal{H}_S &= -\left(\frac{1}{2}\right)\alpha[F + G \cos(\omega t)]^2 \\ &= -\left(\frac{1}{2}\right)\alpha\left\{[F^2 + \left(\frac{1}{2}\right)G^2] + 2FG \cos(\omega t) \right. \\ &\quad \left. + \left(\frac{1}{2}\right)G^2 \cos(2\omega t)\right\} \end{aligned} \quad (4)$$

provided that the frequency is small compared to the p -s

and p - d intervals, the source of the polarizability. The first term is time independent and has the same form as that resulting from imposition of only a dc field on a non-degenerate atomic state. It thus produces a quadratic shift, but in this case the amplitude supplements the effect of F and leads to an ac Stark effect, the energy shift of which is given by

$$\Delta E = \frac{1}{4}\alpha G^2. \quad (5)$$

Note that even if $F=0$, application of the ac field mimics the quadratic dc Stark effect by producing an energy *shift*, a shift proportional to the square of the rms value of the amplitude.

Since the Hamiltonian contains periodic functions of time, we apply Floquet's theorem [7] to solve the time-dependent Schrödinger equation. Taking the solution to be $\Psi(\mathbf{r}, t) = R(\mathbf{r})\psi(t)$, where

$$\psi(t) = \exp\left[-\frac{i}{\hbar}E_a t\right]\phi_{E_a}(t) \quad (6)$$

with

$$\phi_{E_a}(t) = \phi_{E_a}(t + 2\pi/\omega), \quad (7)$$

shows that the ϕ 's may be obtained from a Schrödinger-like eigenvalue equation [4]

$$\left[\mathcal{H}_a - i\hbar\frac{\partial}{\partial t}\right]\phi_{E_a}(t) = E\phi_{E_a}(t). \quad (8)$$

The solutions of Eq. (8) are

$$\begin{aligned} \phi_{E_a}(t) = & \exp\left[-\frac{i}{\hbar}\left\{E_a - \left(\frac{1}{2}\right)\alpha[F^2 + \left(\frac{1}{2}\right)G^2]\right\}t\right] \\ & \times \exp\left[\frac{i}{\hbar}\left[\frac{\alpha FG}{\omega}\right]\sin(\omega t)\right] \\ & \times \exp\left[\frac{i}{\hbar}\left[\frac{\alpha G^2}{8\omega}\right]\sin(2\omega t)\right], \end{aligned} \quad (9)$$

where E_a is the energy of the nondegenerate field-free state, the progenitor state. $R(\mathbf{r})$ is identical to the spatial part of the solution of the Schrödinger equation using only the time-independent part of the Hamiltonian, i.e., \mathcal{H}_a plus the time-independent term in Eq. (4).

The Schrödinger equation takes the form

$$\left[\mathcal{H}_a - i\hbar\frac{\partial}{\partial t}\right]\phi_{E_a}(t) = [E_a + (n\hbar\omega + m2\hbar\omega)]\phi_{E_a}(t), \quad (10)$$

$n, m = 0, \pm 1, \pm 2, \dots,$

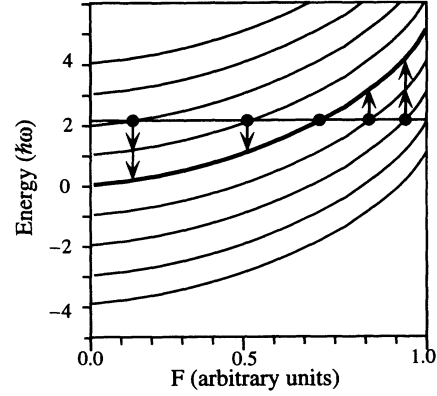


FIG. 2. Schematic diagram of the Floquet states produced by simultaneous application of a dc field F and an ac field of frequency ω . The polarizability has been taken to be negative as for p states of sodium. The progenitor state is represented by the heavy curve. Floquet states that arise from application of only the ac field are the other solid curves and Floquet states that require the presence of both the dc and ac fields are dashed. The energies of all states have been shifted up slightly to emphasize the ac Stark effect.

which shows that here exist two sets of quasienergy, or Floquet, states, one arising from the $\sin(\omega t)$ term and the other the $\sin(2\omega t)$ term. The array from $\sin(\omega t)$ generates Floquet sidebands that are separated by $\hbar\omega$, but only where $F \neq 0$, while that from $\sin(2\omega t)$ produces sidebands separated by $2\hbar\omega$. Figure 2 is a schematic diagram of the quasienergy levels associated with a nondegenerate progenitor level of negative polarizability. The Stark shift in energy is therefore positive. A negative polarizability occurs when the quantum defect (modulo 1) is greater than 0.5, as is the case, for example, for p states of sodium [5].

The horizontal line near $2\hbar\omega$ in Fig. 2 represents the three-photon energy. Floquet F spectra may be envisioned as scans of F across this horizontal line with excitations occurring at intersections of the line with the Floquet states (dots). Alternatively, the excitations to Floquet states lying above the progenitor may be thought of as resulting from absorption by the atom of the three-photon energy plus one or more photons from the ac field (arrows). In this alternate view, excitations to Floquet states lying below the progenitor take place by absorption of the three-photon energy, together with stimulated emission of one or more photons from the ac field.

The previous discussion shows how a set of Floquet states can be excited, but ignores the probability of excitation of a given state. This must be obtained from consideration of the wave function of the system. Rewriting Eq. (9) for the time dependence of the wave function, with the notation

$$\xi = \frac{\alpha GF}{\hbar\omega}, \quad \eta = \frac{\alpha G^2}{8\hbar\omega}, \quad (11)$$

omitting the subscripts, and expanding the exponentials containing sine terms in Fourier series, we have

$$\begin{aligned}\phi(t) &= \exp\left[-\frac{i}{\hbar}(E_a - \varepsilon_{FG})t\right] \sum_{n=-\infty}^{\infty} J_n(\zeta) \exp[i(n\omega t)] \sum_{q=-\infty}^{\infty} J_q(\eta) \exp[i(2q\omega t)] \\ &= \exp\left[-\frac{i}{\hbar}(E_a - \varepsilon_{FG})t\right] \sum_{n=-\infty}^{\infty} \sum_{q=-\infty}^{\infty} J_n(\zeta) J_q(\eta) \exp[i(n+2q)\omega t],\end{aligned}\quad (12)$$

where

$$\varepsilon_{FG} = -\left(\frac{1}{2}\right)\alpha[F^2 + \left(\frac{1}{2}\right)G^2] \quad (13)$$

the dc-like shift in energy of the zero-field state due to the dc field and the rf amplitude. Upon letting $m = n + 2q$ we have [8]

$$\begin{aligned}\phi(t) &= \exp\left[-\frac{i}{\hbar}(E_a - \varepsilon_{FG})t\right] \\ &\quad \times \sum_{m=-\infty}^{\infty} \sum_{q=-\infty}^{\infty} J_{m-2q}(\zeta) J_q(\eta) \exp(imt) \\ &= \exp\left[-\frac{i}{\hbar}(E_a - \varepsilon_{FG})t\right] \sum_{m=-\infty}^{\infty} C_m \exp(imt),\end{aligned}\quad (14)$$

where

$$C_m = \sum_{q=-\infty}^{\infty} J_{m-2q}(\zeta) J_q(\eta). \quad (15)$$

Since the spatial part of the wave function is the same for all Floquet states in this experiment, $|C_m|^2$ is a measure of the probability of excitation of a given Floquet state. Our F spectra should therefore reflect the relative magnitudes of the $|C_m|^2$ at each sideband.

In this paper we illustrate the efficacy of Floquet spectroscopy as a tool for accurately measuring atomic properties by determining the scalar and tensor polarizabilities of the $65p^2P$ state of sodium. The polarizabilities of the fine-structure levels differ, however, as reflected by the different curvatures of the parabolas defining their quadratic energy dependences (at low fields). There are, in fact, three different quadratic states, the energies of which are [9–11]

$$\Delta E = -\frac{1}{2}\alpha_0 F^2 - \frac{1}{2}\alpha_2 \frac{3m_j^2 - j(j+1)}{j(2j-1)} F^2. \quad (16)$$

Figure 3 illustrates the behavior of the fine-structure levels of p states of sodium under the action of the dc field; the $65p$ states are shown because they are observed in our experiments. The energy scale in the drawing is in units of the fine-structure interval of the $65p^2P$ state, ΔE_{FS} , which is 20 ± 10 MHz [2]. The three-photon energy of this experiment has been placed at $6\Delta E_{FS}$, but this placement is equivocal because of the uncertainties of the fine-structure interval as well as the uncertainty in the energy of the $12s^2S$ state, $40482.236 \text{ cm}^{-1} \pm 60$ MHz. Thus the three-photon energy cannot be placed on Fig. 3 with confidence. In fact, we know from the data that it lies several ΔE_{FS} , probably more than six, above the field-free $65p^2P$ energies. Consequently, the $j=3/2$,

$m_j = \pm 3/2$ state (dashed curve) cannot be resolved from the $j=1/2$, $m_j = \pm 1/2$ state (lower solid curve) at the value of F at which they are shifted into resonance. Therefore, in the experiments reported here we observed only the $m_l=0$ and $|m_l|=1$ substates. We therefore write Eq. (16) in the form [11]

$$\Delta E = -\frac{1}{2}\alpha_0 F^2 - \frac{1}{2}\alpha_2 \frac{3m_l^2 - l(l+1)}{l(2l-1)} F^2. \quad (17)$$

Since we are considering only the $65p^2P$ state, identifying subscripts have been omitted. For the two values of m_l we have

$$\Delta E = \begin{cases} -\frac{1}{2}(\alpha_0 - 2\alpha_2)F^2, & m_l = 0 \\ -\frac{1}{2}(\alpha_0 + \alpha_2)F^2, & m_l = \pm 1. \end{cases} \quad (18)$$

It can be seen that if plane polarized laser beams are used, so that only $m_l=0$ final substates are accessed, the data can, at best yield, the coefficient $\alpha = \alpha_0 - 2\alpha_2$. Using circular polarization the CO_2 laser beam, however, permits excitation of both substates and thus the determination of both α_0 and α_2 .

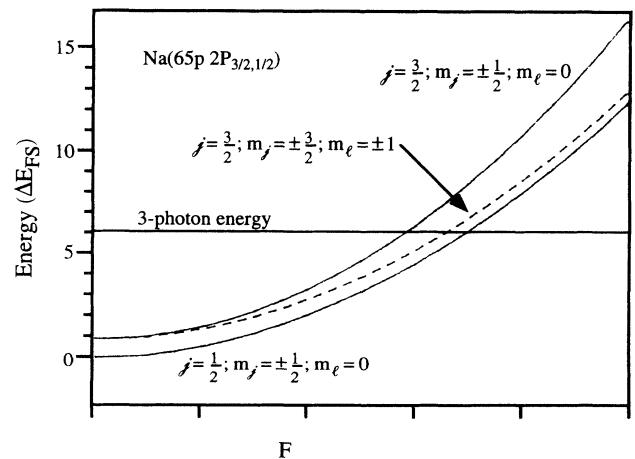


FIG. 3. Diagram showing the splitting of the two fine-structure levels of the $65p^2P$ state of sodium under the influence of an external dc electric field F . The energy units are the fine-structure interval which is known to only within about ± 10 MHz [5]. The horizontal line, which represents the three-photon energy of this experiment, has been placed at approximately 5–6 units above the field-free level, consistent with the data to be presented.

RESULTS AND DISCUSSION

Figure 4 shows an F spectrum obtained with $\omega=400$ MHz using plane polarized $10 P(24)$ radiation from the CO_2 laser. This polarization ensures that only the $j=3/2, m_j=\pm 1/2$ states are excited. The rf amplitude G was adjusted to a value such that the ac Stark shift, Eq. (5), placed the (dc) field-free $65p^2P_{3/2}$ energy barely in excess of the three-photon energy, thus ensuring that this progenitor state would not be present in the F spectrum. Superposed on the F spectrum are the progenitor state and several Floquet sidebands. Note that the energy scale, while uncertain to the degree discussed in the preceding section, is correct with respect to the three-photon energy by virtue of the adjustment of G that placed the progenitor just above the three-photon energy. Moreover, the relative scale is determined by the rf frequency, a quantity that can be routinely set to within ± 100 Hz. In accord with theory, peaks corresponding to excitations occur at values of F such that the sidebands intersect the horizontal line. Further, the intensities are consistent with theory, as evidenced by the bars under the peaks, the heights of which were calculated using Eq. (15).

It is tempting to use the ac Stark shift to compute the value of α [$=-\frac{1}{2}(\alpha_0-2\alpha_2)$] in Eq. (5). It is, however, inconvenient to determine accurately the exact value of G since it must be measured *in situ*, i.e., inside the vacuum system. A better method is one in which the CO_2 laser beam is circularly polarized, thus permitting excitation of both $m_l=0$ and $m_l=\pm 1$ substrates. Floquet spectroscopy permits acquisition of more than one set of data points per F spectrum, thus increasing the precision with which the atomic parameters can be determined. Moreover, using this method both α_0 and α_2 , rather than a linear combination of them, can be determined.

Figure 5 shows 11 F spectra acquired with eight different rf frequency settings; for convenience, these spectra are plotted as signal vs F^2 . In each case the rf amplitude has been adjusted so that the center of the

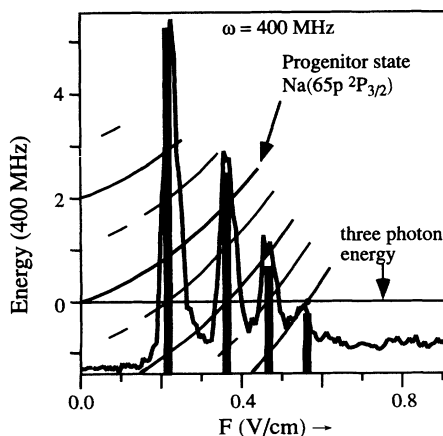


FIG. 4. Floquet F spectrum of the state linked to the $65p^2P_{3/2}(m_j=\pm 1/2)$ state. The progenitor state and several sidebands are shown. The bars represent relative absorption probabilities calculated according to Eq. (15).

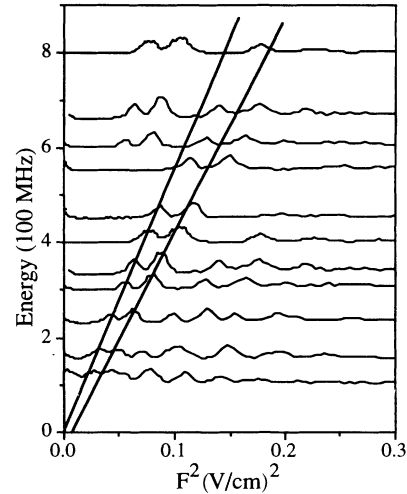


FIG. 5. Floquet F spectra acquired at different rf frequencies plotted versus F^2 . The energy scale is measured from the ac Stark shifted $65p^2P_{3/2}$ state. The spectra are placed at an energy equal to the rf frequency ω , except for energies above 550 MHz, at which the spectra acquired at lower ω were placed at 2ω as explained in the text.

peak corresponding to the lowest-lying progenitor state, the lowest solid curve in Fig. 3, occurs at $F=0$; these peaks have, however, been eliminated from the F spectra to emphasize the sideband peaks. Several spectra have been used twice, an advantage of Floquet spectroscopy. For example, the pair of peaks corresponding to the second Floquet sidebands in the 400-MHz F spectrum provide data at the 800-MHz value of the ordinate.

The fact that the peaks occur in pairs, rather than threes, indicates that the placement of the three-photon energy in Fig. 3 may be too low. Recall that the uncertainty in this placement depends upon the uncertainty in the energy of the 12^2S state, ± 60 MHz, which is roughly 8–10 fine-structure intervals. We can, however, use the polarizabilities that these data yield to adjust the error limits on the $12s^2S$ energy. Determination of polarizabilities by Floquet spectroscopy is independent of the absolute value of the energy.

The fact that the peaks occur in pairs forces us to regard the dashed curve and the lower solid curve in Fig. 3 as coincident at the three-photon energy. The straight lines in the figure clearly show the deviations from quadratic behavior of the quadratic Stark states. Moreover, the deviations are in a direction toward the nearest hydrogenic manifold, which, for sodium p states, is at lower energy.

To obtain the polarizabilities we fit the data, energy E vs F , using a quasi-Newton technique. The fits are displayed in Fig. 6, together with the resulting analytic form of the polynomials. The linear combinations of α_0 and α_2 in the coefficients of F^2 in Eq. (18) are given by

$$-\frac{1}{2}(\alpha_0-2\alpha_2)=\lim_{F \rightarrow 0} \left[\frac{1}{2} \right] \frac{d^2E}{dF^2} = -\frac{1}{2}(\alpha_0+\alpha_2) \quad (19)$$

from which we obtain the values of α_0 and α_2 listed in

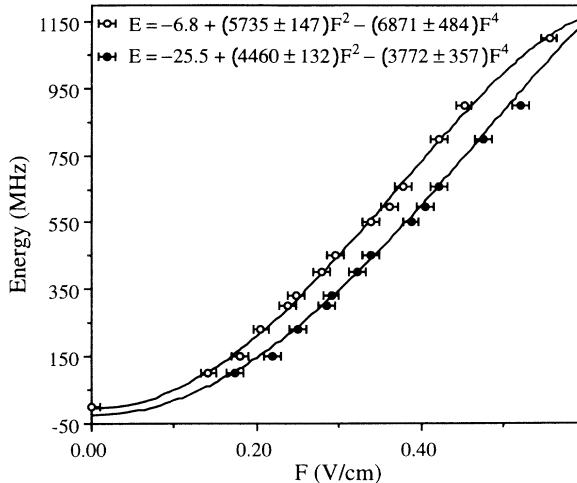


FIG. 6. Data points and curve fits used to obtain the polarizabilities. The equations displayed are those resulting from a fit of the data to an even quartic polynomial. The error bars on the data are based on the half width of the peaks in the Floquet F spectra from which the data were extracted.

Table I. The error limits are suggested by the uncertainties in the data and the curve fitting procedure. Remarkably, these data also lead to a value of the fine-structure interval of 18 ± 5 MHz. This is quite close to the 20 MHz obtained from quantum defects [2] as well as the 20.3 MHz obtained from an extrapolation based on measurements at lower values of n [12]. What is remarkable about our measurement of the fine-structure interval is that fine structure was not even resolved in the experiment.

In spite of these uncertainties, we may, using these values of the polarizability, compute the difference in energy between the field-free $65p^2P$ state and the three-photon energy ΔE_0 . (Recall that determination of α_0 and α_2 did not depend on any absolute energy.) Because this difference depends on the energy of the $12s^2S$ state, we may, based on the present data, redefine the error limits

TABLE I. Polarizabilities of the $65p^2P$ states of sodium obtained in this work.

α_0 [MHz/(V/cm) ²]	α_2 [MHz/(V/cm) ²]
-9770 ± 200	850 ± 200

of that energy. To do this, F was scanned from -0.5 to $+0.5$ V/cm with plane polarized laser beams. Thus only the $65p^2P_{3/2}$ state (with $m_j = \pm 1/2$, $m_l = 0$) could be excited. Because of the symmetric scan in F , two peaks, both corresponding to excitation of this state, were observed. This procedure nulled out any effects of small residual fields at the position of the excitation. At these low fields, ΔE_0 is given to good accuracy by

$$\Delta E_0 = -\frac{1}{2}\alpha F_0^2, \quad (20)$$

where $\alpha = \alpha_0 - 2\alpha_2$, the value for $m_l = 0$, and F_0 is the field at which the peaks occur, 0.187 V/cm. We obtain $\Delta E_0 = 200$ MHz, which may, in view of the uncertainty in ΔE_{FS} , be as much as $10\Delta E_{FS}$. We conclude, therefore, that the ± 60 MHz previously assigned to the $12s^2S$ energy may be revised to $+60$ MHz, minus zero.

Finally, it is of interest to examine the scaling law for polarizabilities, the n dependence of α_0 , using five previously measured values for $23 \leq n \leq 41$ [12], together with our value for $65p^2P$. The polarizability is expected to scale roughly as the seventh power of the principal quantum number. Using the six values at our disposal, we obtain an $n^{7.4}$ dependence, which is quite close to the $n^{7.3}$ power law obtained from theoretical values calculated for principal quantum numbers below $n = 20$ [13].

ACKNOWLEDGMENTS

The authors would like to thank E. Arimondo, T. Bergeman, and T. F. Gallagher for useful comments. We also thank Paul Frederick and Mimi Tarn for technical assistance. The work was supported by the National Science Foundation and the University of Missouri Research Board.

- [1] T. F. Gallagher, *Rydberg Atoms* (Cambridge University Press, Cambridge, 1994).
- [2] M. Ciocca, C. E. Burkhardt, J. J. Leventhal, and T. Bergeman, *Phys. Rev. A* **45**, 4720 (1992).
- [3] S. H. Autler and C. H. Townes, *Phys. Rev.* **100**, 703 (1956).
- [4] See, for example, H. Friedrich, *Theoretical Atomic Physics* (Springer-Verlag, Berlin, 1990), p. 181.
- [5] T. P. Hezel, C. E. Burkhardt, M. Ciocca, L-W. He, and J. J. Leventhal, *Am. J. Phys.* **60**, 329 (1992).
- [6] R. R. Freeman and D. Kleppner, *Phys. Rev. A* **14**, 1614 (1976).
- [7] See, for example, J. Mathews and R. L. Walker, *Mathematical Methods of Physics*, 2nd ed.

- (Benjamin/Cummings, Menlo Park, CA, 1964).
- [8] P. Pillet, R. Kachru, N. H. Tran, W. W. Smith, and T. F. Gallagher, *Phys. Rev. A* **36**, 1132 (1987).
- [9] A. Khadjavi, A. Lurio, and W. Happer, *Phys. Rev.* **167**, 128 (1968).
- [10] T. F. Gallagher, L. M. Humphrey, R. M. Hill, W. E. Cooke, and S. A. Edelstein, *Phys. Rev. A* **15**, 1937 (1977).
- [11] C. Fabre, S. Haroche, and P. Goy, *Phys. Rev. A* **18**, 229 (1978).
- [12] C. Fabre, S. Haroche, and P. Goy, *Phys. Rev. A* **22**, 778 (1980).
- [13] P. F. Gruzdev, G. S. Soloveva, and A. I. Sherstyuk, *Opt. Spektrosk.* **71**, 888 (1991) [*Opt. Spectrosc. (USSR)* **71**, 513 (1992)].

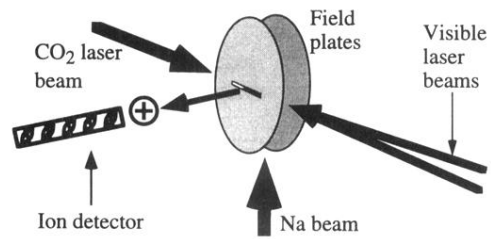


FIG. 1. Schematic diagram of the apparatus.